Acoustics in Moving Inhomogeneous Media

Second Edition

Vladimir E. Ostashev
D. Keith Wilson

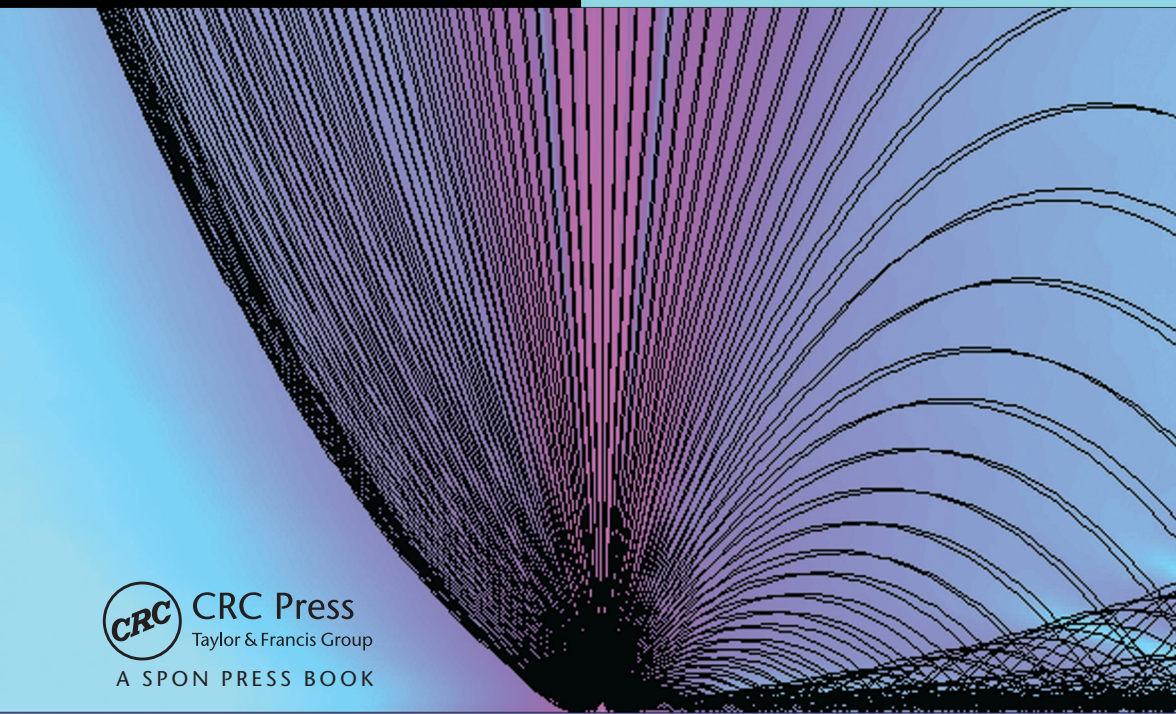

CRC Press
Taylor & Francis Group
A SPON PRESS BOOK

Acoustics in Moving Inhomogeneous Media

Second Edition

Acoustics in Moving Inhomogeneous Media

Second Edition

Vladimir E. Ostashev
University of Colorado, Boulder, Colorado, USA

D. Keith Wilson
US Army ERDC, Hanover, New Hampshire, USA

CRC Press
Taylor & Francis Group
Boca Raton London New York

CRC Press is an imprint of the
Taylor & Francis Group, an **informa** business

A SPON PRESS BOOK

CRC Press
Taylor & Francis Group
6000 Broken Sound Parkway NW, Suite 300
Boca Raton, FL 33487-2742

Version Date: 20150717

International Standard Book Number-13: 978-1-4822-6665-8 (eBook - PDF)

Contents

Preface

This book offers a complete and rigorous study of sound propagation and scattering in moving media with deterministic and random inhomogeneities in the sound speed, density, and medium velocity. This area of research is of great importance in many fields including atmospheric and oceanic acoustics, aeroacoustics, acoustics of turbulent flows, infrasound propagation, noise pollution in the atmosphere, theories of wave propagation, and even astrophysics, with regard to acoustic waves in extraterrestrial atmospheres. Over the past several decades, understanding of acoustics in moving media has grown rapidly, in response to its importance for practical applications such as prediction of sound propagation from highways, airports, and factories; acoustic remote sensing and tomography of the atmosphere and ocean; detection, ranging, and recognition of acoustic sources; and the study of noise emission by nozzles and exhaust pipes.

In the atmosphere, the wind velocity and its fluctuations usually lead to significant changes in sound and infrasound propagation, such as ducting in the downwind direction and scattering into shadow zones. Strong oceanic currents and tides can affect the phase and amplitude of acoustic signals. Sound propagation in gases or fluids are influenced by the mean flow. Propagation of sound waves emitted by moving sources is closely related to acoustics in moving media and is considered in this book. The bulk of the book presents systematic and rigorous formulations of sound propagation in inhomogeneous moving media, which may be applied in many areas of acoustics. Experimental data and numerical predictions considered in the book are pertinent mainly to atmospheric and oceanic acoustics. When studying outdoor sound propagation, the most advanced models for the vertical profiles of temperature and wind velocity and their fluctuations in the atmospheric surface layer and for the ground impedance are used.

Part I of the book considers sound propagation through moving media with deterministic inhomogeneities, such as vertical profiles of temperature and wind velocity in the atmosphere. Chapter 1 presents the history of acoustics in moving media, its applications, typical values of wind and current velocities in the atmosphere and ocean, and their effects on sound propagation. This chapter contains useful background for those new to the subject. In Chapter 2, classical and new equations for sound waves in inhomogeneous moving media are systematically derived from a set of linearized fluid-dynamic equations. This chapter provides appropriate starting equations for solving many particular problems. In Chapter 3, the main results of geometrical acoustics

in an inhomogeneous moving medium are formulated systematically using the Debye series and Hamiltonian formalism. Among these are the law of acoustic energy conservation, the eikonal equation, refraction laws for the sound ray and the normal to the wavefront, and equations for the sound ray path. Geometrical acoustics is particularly useful for the visualization of sound propagation. Chapter 4 deals with the wave theory of sound propagation in stratified moving media (the atmosphere and ocean). The results presented elucidate the effects of the medium motion on propagation of plane and spherical sound waves. Chapter 5 covers the study of sound fields emitted by moving sources. The sound field due to a point source moving with an arbitrary velocity in a homogeneous, motionless medium is analyzed. The bulk of the chapter considers the effects of both source and medium motion on the sound field, such as the Doppler effect and sound aberration in moving media.

The classical theories of wave propagation in media with fluctuations in the sound speed (or light velocity) are well developed and presented in many books. However, in the turbulent atmosphere and ocean, in liquid marine sediments, and in the turbulent flows, the statistical moments of a sound field are affected not only by these fluctuations, but also by the density and medium velocity fluctuations. In Part II, we present rigorous and systematic formulations for the various statistical moments of a sound field propagating in a medium with random inhomogeneities in the sound speed, density, and medium velocity. In Chapter 6, the statistical description of random inhomogeneities in a medium is considered, including most widely used spectra of turbulence. The sound scattering cross section in a turbulent medium is calculated and applied to the analysis of sound scattering in the atmosphere. In Chapter 7, the variances and correlation functions of the phase and log-amplitude fluctuations, the mean sound field, and the mutual coherence function are considered for line-of-sight sound propagation. Multipath sound propagation in a random moving medium is analyzed in Chapter 8. This geometry can occur due to reflection of a sound wave from a surface (e.g., the ground), refraction, or sound scattering at large angles.

Part III describes numerical methods for performing calculations involving equations from the first two parts. Such numerical methods are often needed for practical problems involving sound propagation in the atmosphere, ocean, and other moving media, since the complex and dynamic nature of these environments often prevents the derivation of general, analytical results. Although the example calculations in Part III pertain to outdoor sound propagation near the ground, the techniques can be readily applied to other environments. Techniques for synthesizing realistic random media, as appropriate to wave propagation calculations, are described in Chapter 9. Chapter 10 describes implementation of ray-based methods for the atmosphere, and also provides some background material on boundary conditions for ground surfaces and interaction of sound waves with porous materials. Wave-based methods, in the frequency and time domains, are the subject of Chapters 11 and 12, respectively. The former includes solution of parabolic equations and wavenumber

integration techniques. The emphasis of Chapter 12 is on finite-difference, time-domain (FDTD) calculations. Lastly, in Chapter 13, we explore incorporation of randomness and uncertainty in the outdoor environment (atmosphere and terrain) into propagation calculations.

When writing this book, the authors have endeavored to derive results systematically from first principles. Ranges of applicability are rigorously formulated before interpreting the physical meaning of the results. Such an approach is desirable since heuristic approaches for sound propagation in moving media have, in the past, led to some errors and misconceptions. The main quantities describing sound propagation have the same notation in all chapters of this book. Nevertheless, in each chapter all notations are introduced anew, so that it can be read independently of the other chapters.

This book has been significantly revised and extended from the first edition [290], which was published in 1997. Part I incorporates new results obtained since that time. Part II is significantly rewritten and extended with systematic formulations of sound propagation and scattering in random moving media. Part III, describing numerical methods, is entirely new with this edition.

This book should provide valuable background and a reference resource for engineers and scientists working in industry, government, and military laboratories on research problems involving outdoor noise control, acoustic detection and ranging in the atmosphere, and acoustic remote sensing of the atmosphere and ocean. The step-by-step approach and careful explanations should be useful to teachers and graduate students in universities, polytechnics and technical colleges, in departments of physics, mathematics, earth sciences, and engineering, who are interested in atmospheric and oceanic acoustics, aeroacoustics, acoustics of turbulent flows, outdoor noise, acoustic remote sensing of the atmosphere and ocean, and the theory of wave propagation in inhomogeneous media.

Vladimir Ostashev *Boulder, Colorado*
Keith Wilson *Hanover, New Hampshire*

Biographies

Dr. Vladimir E. Ostashev is a senior research scientist at the Cooperative Institute for Research in Environmental Sciences (CIRES) of the University of Colorado at Boulder (CU) and a government expert for the U.S. Army Engineer Research and Development Center. He earned a PhD in physics from the Moscow Physics and Technology Institute, Russia in 1979. His undergraduate and graduate advisor was Prof. Valerian I. Tatarskii. In 1992, Dr. Ostashev earned a Doctor of physical and mathematical sciences from the Acoustics Institute, Moscow, where his advisor was Prof. Yu. P. Lysanov. Since 1979, he has worked at the Institute of Atmospheric Physics (Moscow, Russia), Acoustics Institute (Moscow, Russia), and New Mexico State University (Las Cruces, New Mexico), before joining CIRES/CU in 2000. Dr. Ostashev has also held visiting positions at the University of Oldenburg (Oldenburg, Germany), Centre Acoustique, École Centrale de Lyon (Écully, France), Open University (Milton Keynes, United Kingdom), and NOAA/Environmental Technology Laboratory (Boulder, Colorado). He is a fellow of the Acoustical Society of America, and an associate editor of the *Journal of the Acoustical Society of America* and *JASA Express Letters*.

Dr. D. Keith Wilson is a research physical scientist with the U.S. Army Engineer Research and Development Center (ERDC), in Hanover, New Hampshire. He earned an M.S. in electrical engineering from the University of Minnesota in 1987, where he was advised by Prof. Robert F. Lambert, and a PhD in acoustics from the Pennsylvania State University in 1992, where he was advised by Prof. Dennis W. Thomson. Dr. Wilson was a research fellow at the Woods Hole Oceanographic Institution under the guidance of Prof. George V. Frisk from 1991–1993, and a research faculty member in the Pennsylvania State University Meteorology Department under Prof. John C. Wyngaard from 1993–1995. He joined the U.S. Army Research Laboratory in 1995 and ERDC in 2002. Dr. Wilson has been awarded U.S. Army Research and Development Achievement Awards on four occasions and received the U.S. Army Meritorious Civilian Service Award in 2012. He is a fellow and recipient of the Lindsay Award of the Acoustical Society of America, associate editor of the *Journal of the Acoustical Society of America*, and founding editor of *JASA Express Letters*. He is a member of the Institute for Noise Control Engineering and the American Meteorological Society.

Acknowledgments

The first edition of this book was prepared for publication with support from the German Acoustical Society, through arrangements by Prof. Volker Mellert (University of Oldenburg, Germany). Frank Gerdes (University of Oldenburg) undertook the printing of the manuscript in LaTeX. Prof. Keith Attenborough (Open University, United Kingdom) read both editions of the manuscript carefully and provided many useful comments. The authors sincerely thank all these people.

Both authors are grateful to their former research advisors for their mentorship, inspiration, and kind support lasting many years: V. Ostashev to Prof. V. I. Tatarskii (formerly with the National Oceanic and Atmospheric Administration) and Prof. Yu. P. Lysanov (deceased), and K. Wilson to Profs. Dennis W. Thomson, John C. Wyngaard, George V. Frisk, Robert F. Lambert, and Kenneth E. Gilbert.

The authors also acknowledge the long-term support of the United States Army, which was facilitated through the Army Research Office, the Engineer Research and Development Center, and the Army Research Laboratory. Indeed, a substantial portion of the research in outdoor sound propagation described in this book, whether conducted by the authors or by others, was sponsored by the U.S. Army.

We hope this book helps to demonstrate the tremendous progress that has been made by the larger research community during the past several decades.

Lastly, but most definitely foremost in mind, the authors are indebted to the unwavering support and patience of their spouses and families during this project.

Part I

Theoretical foundations of acoustics in moving media

In this part of the book, we analyze propagation of sound waves in moving media with deterministic inhomogeneities, such as the vertical profiles of temperature and wind velocity in the atmosphere and synoptic eddies in the ocean. Chapter 1 serves as introduction and acquaints readers with the history of acoustics in a moving medium and its modern applications. Parameters affecting outdoor sound propagation are discussed and a brief overview of atmospheric acoustics is presented. The effects of ocean currents on propagation of sound waves are outlined.

In Chapter 2, equations for acoustic and internal gravity waves in an inhomogeneous moving medium are systematically derived from first principles. An entire chapter is devoted to the derivation of these equations because (i) certain important equations have been obtained only recently, and (ii) the equations for sound waves are often presented in the literature without detailed analysis of their ranges of applicability. These equations are used in the subsequent chapters for analysis of sound propagation.

The main results of geometrical acoustics in an inhomogeneous moving medium are systematically presented in Chapter 3. Starting from a complete set of linearized fluid-dynamic equations, we formulate the law of acoustic energy conservation and derive the eikonal equation, refraction laws for the sound ray and the normal to the wavefront, and the equations for sound ray paths. The ray paths are particularly helpful in visualizing sound propagation. Examples of ray tracing in the atmosphere and ocean are presented.

Geometrical acoustics does not enable one to describe diffraction of sound waves and is not applicable to relatively low frequencies. These difficulties can be overcome with the wave theory of sound propagation in a stratified moving medium, which is considered in Chapter 4. This is a rigorous theory, which has a wider range of applicability than the effective sound speed approximation. The results in this chapter describe the effects of medium motion on the sound-pressure field.

Chapter 5 deals with the analysis of the sound fields emitted by moving sources and observed by moving receivers. The chapter begins with the study of the sound field of a point source moving with an arbitrary velocity in a homogeneous motionless medium. Then, the effects of source, receiver, and medium motion on the sound field are analyzed. In particular, sound aberration and the Doppler effect in an inhomogeneous moving medium are considered.

1

Introduction to acoustics in a moving medium

This introductory chapter begins our journey through the subject of acoustics in moving media: its history, theory, computational methods, and applications. By *moving media*, we mean a medium with an ambient flow; that is, a fluid in motion *prior* to the introduction of a sound wave. Such motion is called the *wind* in the atmosphere, or the *current* in the ocean. But, much of the underlying science applies to media other than the ocean or atmosphere, such as wave propagation through flows of fluids. In addition to winds and currents, the fluid motions may include random disturbances such as *turbulence* and *internal waves*.

Section 1.1 acquaints readers with the history of acoustics in a moving medium and with its modern applications. A brief overview of atmospheric acoustics follows in section 1.2. This section also describes parameters affecting sound propagation in the atmosphere, such as the vertical profiles of temperature and wind velocity. In section 1.3, the parameters of ocean currents are briefly overviewed and some experimental and theoretical results on sound propagation in the ocean with currents are presented. The subsequent chapters, where the theory of sound propagation in inhomogeneous moving media is systematically presented, also contain some historical perspectives, experimental data, and numerical results, but more specifically related to the subject of the chapter.

1.1 Historical review

Throughout this book, and particularly with regard to the following historical discussion, we endeavor to present the subject of acoustics in moving media based on the primary, original papers. Two review papers [26, 93], and the historical review sections found in references [52, 71, 76, 151], were primary references enabling us to connect the threads among the original papers on this subject.

1.1.1 First papers on acoustics in a moving medium

The study of acoustics in a moving medium initially emerged from interest in sound propagation in the atmosphere. Long before the advent of modern science, it had been observed that sound appeared to be louder downwind than upwind from a source. This phenomenon was also evident in the first experiments on sound propagation in the atmosphere, such as those performed by Delaroche [95] and Arago [8]. A correct qualitative explanation of this phenomenon was not provided, however, until 1857 by Stokes [366]. Since the wind velocity should increase with height in the near-ground atmosphere, sound propagating upwind bends upward and thus can pass over the head of an observer, who is then said to be in an acoustic shadow zone (in analogy to an optical shadow). But, in the downwind direction, the sound bends downward, so that the observer is in an insonified zone. (The ray paths for sound propagation downwind and upwind are illustrated in figures 3.4 and 3.5 of Chapter 3.)

Nearly the same explanation for the distinct audibility in the downwind and upwind directions was given by Reynolds [329], seventeen years after Stokes. But, unlike Stokes, Reynolds used the concept of sound rays for this explanation. Reynolds also verified experimentally Stokes's assumption that the bending of sound (a sound ray, according to Reynolds) upwind causes a decrease in audibility. In his experiments, the height below which no sound was heard was measured. Reynolds's experiments confirmed that the greater the distance from the source to the receiver, the greater this height. Furthermore, Reynolds assumed [329], and then verified experimentally [330], that a sound ray bends upward if the temperature decreases with height. This allowed Reynolds to explain why sound from a particular source can be heard better at night than in the daytime. In the daytime, the temperature and, hence, the speed of sound decreases with height, so that the paths of sound rays turn upward, similarly to sound traveling upwind. On the other hand, at night in the near-ground atmosphere, the temperature usually increases with height and the sound rays turn downward, as in propagation downwind. Independently of the study done by Reynolds, and practically at the same time, the effect of wind on sound propagation in the atmosphere was studied experimentally by Henry [164]. Based on his experimental results, Henry concluded that sound propagation is affected significantly by refraction due to wind velocity stratification.

Rayleigh [324] developed the first mathematical description of sound propagation in moving media and formulated the refraction law governing the normal to the wavefront in a stratified moving atmosphere. Using this law, he derived an equation for the ray path. However, Rayleigh's derivation was later recognized to be incomplete, because it did not distinguish between the unit vector $\mathbf{n}$ normal to the wavefront and the unit vector $\mathbf{s}$ tangential to the ray path. Barton [23] was the first to show that these vectors do not generally coincide in a moving medium. Barton also formulated a rule for calculating

the group velocity of a sound wave propagating in a stratified atmosphere. Using this rule, Barton calculated the sound ray paths. While many papers on acoustics in moving media have pointed out Rayleigh's mistake, he was the first to formulate the refraction law for the normal **n** to the wavefront in a moving medium. Moreover, the distinction between the vectors **n** and **s** had not been made prior to Rayleigh; by revealing their difference, Barton made a key contribution to the development of acoustics in a moving medium.

Further development of this field of acoustics was motivated by two practical problems. First, for detection and ranging of artillery and airplanes, the corrections due to refraction of sound waves in the inhomogeneous atmosphere had to be obtained. This problem was considered in detail by Milne [253] in 1921, who revised formulas for calculating the refraction corrections. Furthermore, Milne presented the equations for the phase and group velocities of a sound wave in a three-dimensional moving medium, and also for the ray path. Detection and ranging of artillery and airplanes remained an important application in atmospheric acoustics until the end of World War II. Another important application was the study of sound propagation from large explosions, which resulted in the development of geometrical acoustics for moving media.

1.1.2 Sound propagation from large explosions

In 1904, Borne [40] was the first to detect so-called abnormal propagation of sound in the atmosphere produced by large explosions on the earth's surface. It follows from the observations by Borne and many others (see references cited in [76, 103, 277]) that the sound waves from large explosions, propagating at small elevation angles with respect to the horizon, have turning points in the upper atmosphere. The sound waves then return to the earth's surface, but at large horizontal distances from the explosive source. Therefore, a zone of silence occurs between the initial zone of audibility near the source, and the one resulting from the upper atmosphere return. The term *abnormal sound propagation* was widely used in the first half of the 20th century to describe this phenomenon, but is seldom used nowadays. Sound signals from supersonic aircrafts, rocket launches, and volcanic eruptions can also have turning points in the upper atmosphere and propagate over long ranges.

Analysis of the acoustic travel time from large explosions has shown that turning points for the sound waves can occur in the troposphere, near the ozone layer in the stratosphere at a height of 40–50 km, or in the thermosphere at a height above 100 km. Sound signals with turning points in the troposphere can propagate over long ranges. Such sound signals have been recorded reliably at a horizontal range of 500 km from a source [103]. The cause of sound propagation of this type is the increase in wind velocity $v(z)$ with the height z in the troposphere, which results in downward refraction. A waveguide is formed between the turning points of sound waves and the earth's surface, thus enabling long-range propagation of low frequency signals.

In the thermosphere, the temperature $T(z)$ rapidly increases with height. As a result, sound signals from large explosions propagating at certain elevation angles can have turning points in the thermosphere and return back to the earth's surface. Sound signals with turning points in the stratosphere are considered in the next subsection.

Interest in sound propagation from large explosions declined significantly after World War II because of the use of rockets in studies of the upper atmosphere. Nevertheless, some research in this area continued [7, 32, 85]. Remote sensing of the upper atmosphere by sound signals from large explosions on the earth's surface was a part of the "Mass" project carried out in the USSR in the 1980s [4, 59, 60]. Sound signals from the supersonic Concorde aircraft, which had the turning points in the thermosphere, were recorded at horizontal ranges from 165 km to 10^4 km [21]. Sound propagating through the upper atmosphere can also be used to detect and range nuclear explosions [311, 315]. In the mid-1990s, a network of 60 infrasound stations located worldwide was designed to comply with the Comprehensive Nuclear Test Ban Treaty. This has renewed interest in sound and infrasound propagation in the upper atmosphere [219].

1.1.3 Sound signals with turning points in the stratosphere

In this subsection, we consider only sound propagation from large explosions which have turning points in the stratosphere. Initially, many different explanations were suggested for the observed properties of sound propagation from large explosions; for example, by Obolenskii [277]. In 1912, Fujiwhara [124, 125] was the first to suggest that the observations could be explained by refraction from wind stratification in the upper atmosphere. For arbitrary profiles of the sound speed $c(z)$ in a motionless medium and the wind velocity $\mathbf{v}(z)$, Fujiwhara derived the equation of a sound ray and obtained the height z_t of the turning point, the travel time along the path, and the location of the audibility zones. Working independently and using a different approach, six years later, Emden [108] rederived the equations obtained by Fujiwhara, and calculated the sound ray paths for various profiles of $c(z)$ and $\mathbf{v}(z)$. The papers by Fujiwhara and Emden showed clearly that the effects of wind stratification $\mathbf{v}(z)$ on the refraction of sound in the atmosphere are significant. However, stratification of $\mathbf{v}(z)$ cannot by itself explain the turning points of sound signals in the stratosphere, because the zones of audibility often have an appearance similar to a ring [103, 277].

By the end of the 1930s, the turning points in the stratosphere were usually attributed to the increase in the sound speed $c(z)$ in the stratosphere, causing refraction of sound rays and their return to the ground. In the stratosphere, sound ray paths can be obtained from Snell's law: $c(z)/\cos\theta(z) = \text{constant}$. Here, θ is the elevation angle (the angle between the direction of ray propagation and the horizontal plane), and the sound speed $c(z)$ is related to the temperature $T(z)$ by equation (1.1) below. It follows from this equation and

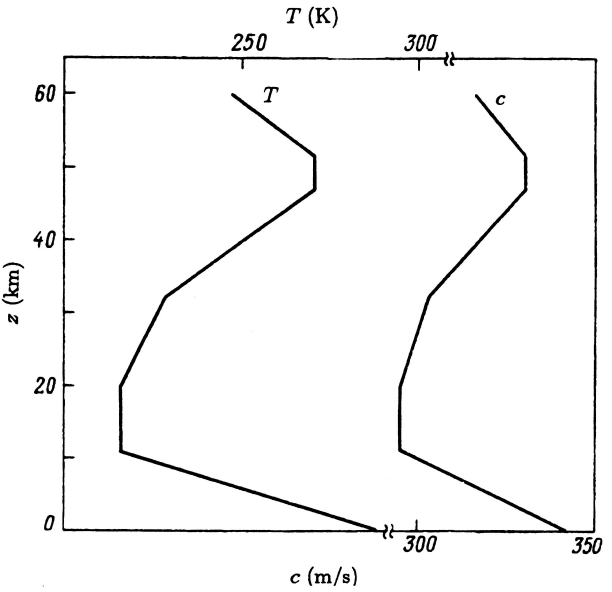

FIGURE 1.1
Vertical profiles of the temperature $T(z)$ and sound speed $c(z)$ of the standard atmosphere [365].

Snell's law, that a sound wave can have a turning point at a height z_t only if $c(z_t) > c(z = 0)$ and, hence, $T(z_t) > T(z = 0)$.

In the decades preceding World War II, sound propagation from large explosions was studied extensively. Hundreds of explosions on the earth's surface were made in many European countries [103]. Tens and sometimes hundreds of observers situated at different distances and azimuthal directions measured the travel time t_{tr} of sound propagation from the point of explosion to the point of observation. Such an interest in sound propagation in the upper atmosphere arose from the fact that direct measurements of temperature and wind velocity were not possible at heights above 20 km at that time. Therefore, scientists endeavored to reconstruct the vertical profiles of $c(z)$ and $T(z)$ from the measured travel times t_{tr} and the angles at which the sound wave arrived at the earth's surface, while usually assuming that $\mathbf{v} = 0$. The vertical profiles of $c(z)$, reconstructed by this method, indicated that at heights of 40–50 km the sound speed was much greater than its value $c(z = 0)$ near the ground (see, for example, references [103, 277]). But this height dependence of the sound speed differs qualitatively from that in the standard atmosphere [365] obtained using rocket data, as shown in figure 1.1. In the standard atmosphere $c(z) < c(z = 0)$ at heights $z \sim$ 40–50 km so that, according to Snell's law, sound waves cannot have turning points (at least, in the upwind direction).

Thus, in the 1920s and 1930s, the vertical profiles of $c(z)$ and $T(z)$ in the stratosphere were not reconstructed correctly, and all causes of the return of sound signals from the stratosphere were not identified. Nevertheless, the study of sound propagation in the upper atmosphere did lead to many important new results for geometrical acoustics in a moving medium. Recent studies [80] explain the return of sound and infrasound signals from the stratosphere as scattering from the fine structure of the temperature and wind velocity fields when random inhomogeneities are significantly elongated in a horizontal direction.

1.1.4 Current applications of acoustics in a moving medium

Interest in atmospheric acoustics, and acoustics of moving media in general, was significantly reduced after World War II, because electromagnetic waves then became widely used for purposes such as detection and ranging, direction finding, and sounding. But, by the beginning of the 1970s, interest in acoustic methods reemerged in many fields of physics. This subsection describes many of the current applications where the theories of wave propagation in moving media are used.

Important applications of atmospheric acoustics include detection, recognition, and tracking of sound sources using microphone arrays; broadcasting over long ranges (loudspeakers can be installed near the ground and also on airplanes and helicopters); and prediction of sound propagation near the ground, given the temperature and wind velocity fields, terrain, and the properties of the ground. The latter is important in predicting noise levels near highways [328], railways [390], and airports [352], the peak and mean sound-pressure levels from small explosions and gunfire [148, 195], and in other practical concerns. The effect of temperature and wind velocity fluctuations on the rise time and shape of sonic booms has been examined [42, 312], as these relate to the annoyance of sonic booms from supersonic passenger aircraft, and aircraft designs to mitigate such annoyance.

Since the beginning of the 1970s, acoustic and radio-acoustic remote sensing techniques have rapidly evolved and entered into widespread usage for measuring the structure of the lower atmosphere [44]. These techniques are enabled by theories of wave propagation in moving media (section 6.4), which relate the sensed signals to atmospheric parameters. Acoustic and radio-acoustic sounding are also significantly affected by refraction of sound in the atmosphere. For example, the maximum height of radio-acoustic sounding is restricted mainly by sound beam advection due to the horizontal wind [188, 192]. Refraction of sound due to temperature and wind velocity stratification can affect acoustic sounding in the atmosphere [43, 134, 309, 310]. Some proposed techniques for remote sensing of the temperature of the atmosphere and the vertical profiles of the sound speed in the ocean are based on the refraction of sound [53, 290].

Acoustic tomography, including diffraction tomography [337], applied to

the ocean [266, 267], the atmosphere [433], and other moving media, is a remote sensing technique for reconstruction of the sound speed and medium velocity fields. Acoustic travel-time tomography of the atmospheric surface layer is considered in Chapter 3.

Aeroacoustics, which deals with the radiation and propagation of sound waves due to aerodynamic forces and unsteady flows, is usually considered to be a field of acoustics distinct from the acoustics of moving media. However, the fields do have some overlapping research goals, such as investigation of the effects of the mean profile of a turbulent jet on the emission of sound waves [144].

Acoustics in moving media also pertains to studies of sound propagation in ducts, nozzles, and diffusers with gas flow [61, 166, 263, 265, 371]. This is relevant, for example, to the analysis of noise emitted by nozzles and exhaust pipes, and the stability of propellant combustion in rocket engines.

Until the beginning of the 1970s, the effects of currents on sound propagation in the ocean had usually been ignored. However, recent theoretical and experimental results have shown that in certain cases, currents can affect the sound field in the ocean quite significantly. (See section 1.3.)

Acoustics of inhomogeneous moving media has applications in astrophysics when studying acoustic and gravity waves in the solar atmosphere in the presence of laminar or random flows, e.g., references [268, 269].

1.2 Sound propagation in the atmosphere

In this section, parameters affecting sound propagation in the air are considered. The approximation of the effective sound speed, which is used widely in atmospheric acoustics, is introduced and discussed. A brief overview of near-ground sound propagation is presented.

1.2.1 Parameters affecting sound propagation in the air

Sound waves propagating in the atmosphere are attenuated by relaxation and dissipation processes in air. These phenomena have been well studied [52, 368]; the resulting absorption coefficient depends on the temperature, humidity, acoustic frequency, and, to a lesser extent, on atmospheric pressure.

Propagation of sound is also affected by the sound speed c and wind velocity $\mathbf{v}$. As will be derived later in this book (equation (6.84)), the sound speed in the atmosphere is given by

$$c = \sqrt{\gamma_a R_a T\,(1 + 0.511q)}. \tag{1.1}$$

Here, $\gamma_a = 1.40$ is the ratio of specific heats for dry air, $R_a = 287.058\ \mathrm{m}^2/(\mathrm{s}^2\,\mathrm{K})$ is the gas constant for dry air, and q is specific humidity.

It follows from equation (1.1) that the sound speed c is primarily affected by temperature T, while the effect of humidity on c is smaller, but not necessarily negligible.

The temperature T, humidity q, and wind velocity $\mathbf{v}$ are among the most important parameters affecting sound propagation. Both their mean values and fluctuating components are important. The fluctuations in T, q, and $\mathbf{v}$ and their effect on sound propagation are studied in detail in Part II of this book. It is often reasonable, for modeling purposes, to view the atmosphere as a stratified, moving medium in which T, q, and $\mathbf{v}$ depend only on the vertical coordinate z. We refer to these quantities as the mean *vertical profiles*. The horizontal component of the vector $\mathbf{v}$ is usually much greater than its vertical component, which is thus often assumed to be zero.

The vertical profiles of $T(z)$, $q(z)$, and $\mathbf{v}(z)$ in the atmospheric surface layer (ASL) have been studied extensively. For neutral or unstable stratification, the ASL extends vertically to about 100–200 m from the ground; for stable stratification, the top of the ASL is usually lower. In the ASL, the vertical profiles of temperature, humidity, and wind velocity can be determined with the Monin–Obukhov similarity theory (MOST), which is considered in section 2.2.3.

Above the ASL (in the atmospheric boundary layer and free troposphere), these profiles can be obtained using direct measurements with weather balloons (tethersondes and radiosondes) and airplanes, and with the numerical weather prediction (NWP) computer models, such as the Weather Research and Forecasting (WRF) Model, which was developed through a collaboration of multiple organizations in the United States, or the European Centre for Medium-Range Weather Forecasts (ECMWF) Integrated Forecast System. NWP is improving in accuracy and resolution as a result of advances in numerical methods and computational hardware.

Jet flows often appear in the stratosphere and upper troposphere [245]. The height of the axis of the jet flows is about 10 km in the middle latitudes. The vertical and horizontal scales of the jet flow and the wind velocity on its axis vary significantly; the characteristic values of these quantities are 10 km, 1500 km, and 50 m/s, respectively. The wind velocity can reach a value of 200 m/s on the axis of the jet flow, corresponding to the Mach number $M = v/c \sim 0.6$.

The mean profiles of wind velocity and wind direction in January and July at latitude 30° are presented in figures 1.2 and 1.3 [146, 189]. These figures indicate that, in the stratosphere, the wind velocity reaches a few tens of meters per second and the wind direction can significantly vary with height. The vertical profile of the temperature in the standard atmosphere [365] is shown in figure 1.1. Significant spatial-temporal variability in the temperature and wind velocity in the atmosphere is caused by its general circulation, the seasonal modulations, and the day-to-day variations due to planetary waves and eddies, the tides produced by solar heating, and internal gravity waves [90].

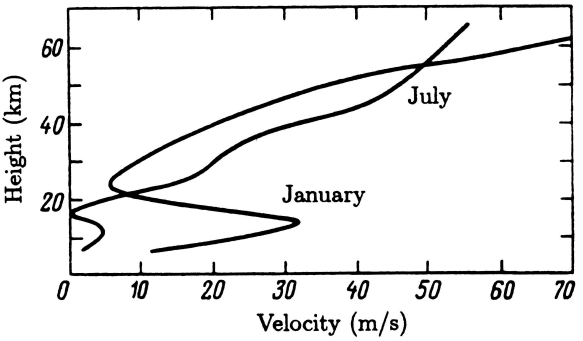

FIGURE 1.2
Vertical profiles of wind speed in January and July at latitude 30° [189, 146].

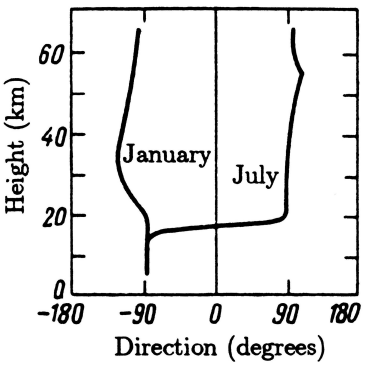

FIGURE 1.3
Vertical profiles of wind direction in January and July at latitude 30° [189, 146].

1.2.2 Effective sound speed approximation

Approximations are commonly employed to represent sound propagation through a moving medium using an effective, motionless medium. The most common of these is the effective sound speed approximation, which involves setting the sound speed to

$$c_{\text{eff}} = c + \mathbf{s} \cdot \mathbf{v}. \tag{1.2}$$

Here, $\mathbf{s}$ is the unit vector tangential to the sound ray path. This approximation was introduced by Rayleigh [324] and is still employed in atmospheric acoustics, ocean acoustics, and acoustics of tubes with flow. With this ap-

proximation, many analytical and numerical methods developed for acoustics in a motionless medium can be applied to a moving medium.

For sound propagation near the ground, the elevation angle of the vector **s** is usually small. In this case, the effective sound speed is often used in the following form

$$c_{\text{eff}} = c + v\cos\psi. \tag{1.3}$$

Here, ψ is the angle between the azimuthal direction of sound propagation and the horizontal wind velocity **v**.

It must be kept in mind that the effective sound speed approximation is a heuristic approach, which cannot describe many important effects that a moving medium has on sound propagation. The ranges of applicability of this approximation are studied in reference [139]. In particular, it is shown that this approximation is valid for calculations of the sound-pressure field only if $v/c \ll 1$, so that terms of order $(v/c)^2$ can be ignored. Other assumptions might also apply for this approximation to be valid [139].

As an example of the limitations of the effective sound speed approximation, note that, in a stratified moving medium, the actual sound ray path is generally a three-dimensional curve, even if it is calculated to order $O(v/c)$. On the other hand, with the effective sound speed, a ray path is always a two-dimensional curve. (This result does not contradict the ranges of applicability of this approximation obtained in reference [139], since a ray path is not directly related to the sound field.)

In this book, sound propagation in a moving medium is studied from first principles rather than with the effective sound speed approximation. In some approximate equations derived from the exact equations, the sound speed and medium velocity can be combined into c_{eff}. In addition to c_{eff}, the effective density ϱ_{eff} might be needed to approximately replace sound propagation in a moving medium with that in a motionless medium with c_{eff} and ϱ_{eff}. The effective density is considered in section 4.1. It has been used in the literature to a much lesser extent than the effective sound speed.

1.2.3 Sound propagation near the ground

Among the sources of acoustic waves propagating near the ground are cars, trains, aircraft, working factories, wind turbines, shots from artillery and small arms, and explosions. Sound from these sources can be heard or recorded at distances up to a few kilometers along the earth's surface. The frequency range of interest is typically from about 10 Hz up to a few kHz, as sound at higher frequencies is strongly attenuated by the air.

Propagation above a partially reflecting (impedance) ground has been studied extensively [16]. Analytical solutions are available for the case of a homogeneous atmosphere above flat ground. The solution is conveniently formulated as a complex image source, with corrections for spherical wave reflection [15, 106]. Extensions incorporate decorrelation between direct and

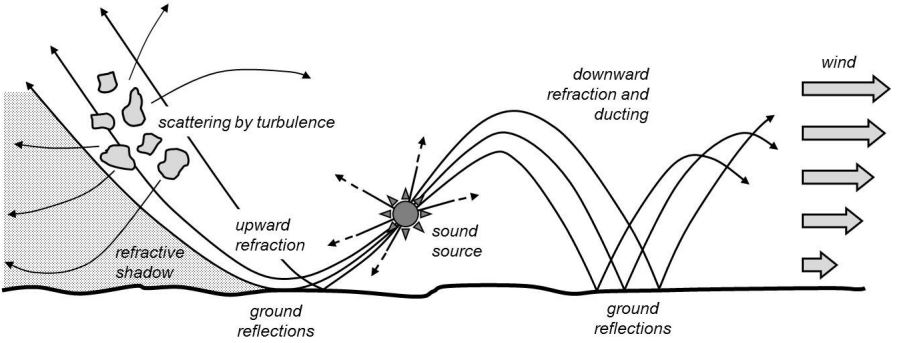

FIGURE 1.4
Outdoor sound propagation phenomena and their interactions.

ground-reflected ray paths resulting from turbulence [82, 86, 297, 347]. This phenomenon raises sound levels above what would normally be observed at locations where the direct and reflected rays interfere destructively.

The many complex effects of weather and terrain on outdoor sound propagation present great challenges for modeling. Refraction and turbulent scattering in the atmosphere vary dramatically in response to changing solar radiation and wind conditions. Sound waves interact with hills, man-made structures such as buildings, natural landcover cover (vegetation), soil, and near-surface geology. Landcover and elevation changes also locally modify the atmospheric flow, which in turn affects the propagation. Many of these interacting phenomena are illustrated in figure 1.4. Although this book, since it deals with the acoustics of moving media, addresses primarily the refraction and scattering effects, in Part III we also discuss numerical modeling of some other phenomena of interest.

1.2.3.1 Atmospheric stratification

Of particular importance for sound propagation is the stratification of the temperature and wind velocity fields, which leads to strong vertical gradients and the refraction of the sound. In the near-ground atmosphere, the temperature $T(z)$ and wind speed $v(z)$ profiles can be determined with MOST; see equations (2.45) and (2.44), respectively. The refraction effects can be most simply understood in terms of the effective sound speed c_{eff} defined with equation (1.3). A positive gradient in c_{eff} leads to downward refraction of sound, which normally enhances sound levels near the surface, whereas a negative gradient leads to upward refraction, which normally diminishes sound levels.

A negative vertical gradient, and hence upward refraction, may be caused by either a temperature lapse condition, which means that the temperature (and hence the sound speed) decreases with height, or by a negative wind shear. Negative wind shear (decreasing wind velocity with height) usually

occurs in the upwind direction, meaning that the wind is blowing from the receiver to the source. A positive vertical gradient and downward refraction may be caused either by a temperature inversion condition, which means that the temperature increases with height, or by a positive wind shear, which usually occurs in the downwind direction. The temperature gradient and wind shear effects are both important, in general. Depending on the atmospheric state and propagation direction, they may combine to strengthen or diminish the overall refractive effect.

As mentioned, downward refraction is normally associated with enhanced sound levels, whereas upward refraction is associated with diminished levels. However, these expectations do not always hold. For example, sound levels may actually be elevated near the boundary of a refractive shadow zone, due to the presence of a caustic there. Downward refraction conditions are complicated by interference effects between ray paths or propagating modes, and by interactions between ducted sound and absorbing ground surfaces.

Given the importance of vertical refraction of sound in the near-ground atmosphere, it is important that propagation calculations incorporate this effect. Ray-based methods can calculate refraction very efficiently, and are also very helpful in visualizing propagation phenomena. Chapter 3 provides ray acoustics equations that correctly incorporate the effect of wind on refraction, whereas Chapter 9 describes the numerical solution of these equations.

The main drawback of ray acoustics is its unsuitability for low frequencies. Ordinary ray methods also do not describe diffraction and scattering into shadow regions, as occurs during strong upward refraction. The fast-field program (FFP) and parabolic equation (PE), which were introduced into atmospheric acoustics in the late 1980s, largely avoid the drawbacks of ray-tracing methods. The FFP [220, 411] solves a Helmholtz type equation (see sections 2.3 and 4.1) which has been Fourier-transformed with respect to the horizontal coordinates. The vertical coordinate is partitioned into a finite number of layers. The PE [137, 403] is based on a finite-angle (forward propagating) approximation to the full wave equation. Derivations of narrow-angle and wide-angle PEs are presented in section 2.5. A starting condition at the source is marched forward in the horizontal range coordinate. Chapter 11 further describes the numerical implementation of the FFP and PE and provides example calculations for sound propagation in the atmosphere.

Recently, there has been strong interest in finite-difference, time-domain (FDTD) methods, due to their ability to readily handle many complex signal generation and propagation phenomena. Refraction can be rigorously incorporated in FDTD calculations [38, 303]. Equations appropriate to FDTD calculations in a moving medium are derived in section 2.4, whereas their numerical solution is described in Chapter 11.

1.2.3.2 Turbulence

The lower atmosphere contains random motions on a variety of scales. Most of these motions are *turbulent*; that is, three-dimensional, rotational disturbances of temperature and wind velocity. Atmospheric turbulence is generated by wind shear, and by buoyancy instabilities resulting from unstable stratification. Large turbulent eddies span the depth of the atmospheric boundary layer, which is up to roughly 2 km thick, and have time scales of many minutes, whereas the smallest eddies have sizes less than 1 cm and produce variations shorter than 1 s. Therefore, the sound field also undergoes random variations on these time scales. While stable stratification suppresses turbulence, internal gravity waves are common in such conditions.

Atmospheric turbulence leads to scattering of sound energy into refractive shadow zones, amplitude and phase fluctuations in received sound signals, fluctuations in the angle of arrival, coherence loss, and changes in the interference pattern between the direct and ground-reflected waves. These effects are important for studies of noise propagation in the atmosphere, source localization with phased sensor arrays, and remote sensing techniques such as acoustic and radio-acoustic sounding.

Representation of the turbulence is often a major challenge. Ideally, we can derive closed-form equations for the sound-field statistics of interest (as considered in detail in Part II of this book), as this approach often enables a better understanding of the physics of the problem and can lead to faster numerical calculations. Such analytical results also aid the development of remote sensing techniques. However, suitable equations for the spectrum of the turbulence are still required. Alternatively, for numerical calculations, we may consider using a computational fluid dynamics (CFD) simulation, or synthesizing the turbulence kinematically. The relative benefits of these approaches are described in Chapter 9, which also discusses kinematic methods in detail, since they are widely used in outdoor sound propagation. Typically, numerical calculations are performed by a Monte Carlo approach, in which a sound field propagates through many realizations of the turbulence field.

1.2.3.3 Uncertainties in predictions

A useful analogy can be made between predicting sound propagation outdoors and predicting the weather. Weather forecasts are imperfect because the numerical forecast models are initialized with atmospheric observations that do not describe the atmospheric state with full accuracy and resolution. The forecast models themselves have a finite resolution and do not perfectly capture the atmospheric physics. Similarly, solutions for outdoor sound propagation are based on imperfect knowledge of the environment (natural and man-made ground cover, building materials, atmospheric wind and temperature profiles, terrain elevation variations, etc.) and cannot capture all of the pertinent physics, such as scattering from small-scale turbulence and vegetation, and coupling of vibrations into the ground.

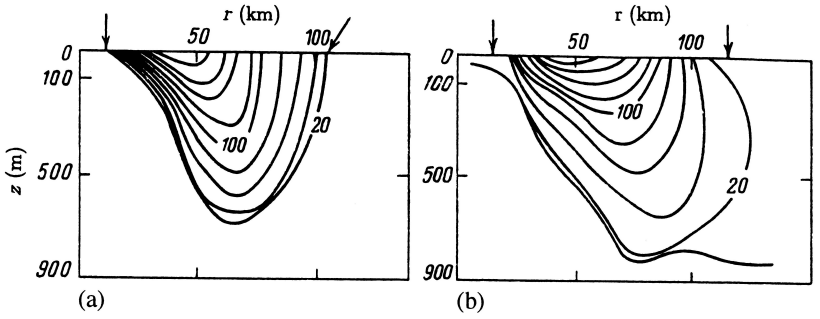

FIGURE 1.5
Isotachs of the Gulf Stream in vertical planes in two locations. (a) $(60°09', 27°26')$ May–June 1967; (b) $(80°24', 30°20')$ July–August 1967 [333].

Uncertainties may be attributed to both the model itself, and to the model parameters. The literature on outdoor sound propagation modeling has typically focused on the former source of uncertainty, namely improving models to handle more complex physics and to improve numerical methods. However, numerical methods for sound propagation can be employed much more effectively when their predictive capabilities, relative to the inputs provided to them and the uncertainties inherent to sound propagation, are well understood. This topic is the primary concern of Chapter 13, which considers application of stochastic integration to problems involving sound propagation in the presence of refraction and turbulence.

1.3 Effects of currents on sound propagation in the ocean

1.3.1 Motion of oceanic water

Many types of motion occur in ocean waters. We consider here only the most typical types [91, 260].

The strongest currents in the world are the Antarctic circle current, the Gulf Stream, the Kurocio current, and Cromwell's current. The characteristic parameters of these currents are nearly constant in space and time. The vertical velocity of a current is much smaller than the horizontal velocity and is usually ignored in oceanic acoustics. The maximum velocity of currents reaches a value of 1.5–2 m/s.

Figure 1.5 shows isotachs of the velocity v of currents in the Gulf Stream measured in vertical planes perpendicular to the current axis at two locations [333]. The arrows indicate the horizontal range r at which the mean velocity

of the current on the ocean surface is zero and z is the depth. The figure indicates that the current velocity has its maximum on the surface and the current does not reach the oceanic bottom. Although this dependence of v on z is typical for some other currents, this is not the case for all currents. For instance, the Antarctic current reaches the bottom, and the velocity of Cromwell's current has its maximum at a depth of 100–200 m in the eastern part of the Pacific Ocean.

Usually, the vertical profiles of currents have fine structure. The fine structure is caused by horizontal layers existing everywhere in the ocean, with nearly constant values of the sound speed c, temperature T, and velocity $\mathbf{v}$ in the layers and large vertical gradients of these functions near their boundaries. The vertical scales of the layers range from ten centimeters to few tens of meters. The horizontal scales are up to tens of kilometers, and they exist from a few hours to a few days. Near the boundaries of the layers, the vertical gradients of the current velocities are much greater than those in the layers and can reach a value of 5–10 cm/s per meter. The fine structure of the current velocity measured by a quick-response probe is seen clearly in figure 1.6 [260].

Synoptic eddies are unsteady objects in the ocean analogous to cyclones and anticyclones in the atmosphere. The synoptic eddies are usually subdivided into the eddies of the open ocean and the frontal eddies generated by frontal currents. For example, 5–8 cyclonic and anticyclonic frontal eddies typically break away each year from the Gulf Stream. In the Northern Hemisphere, the cyclonic eddies rotate anticlockwise and contain cold water relative to the surrounding water. The anticyclonic eddies contain warm water and rotate clockwise. The characteristic scales of the frontal eddies range from 100 km to 400 km, the mean velocity of the eddy center is of the order of a few cm/s, and the maximum velocity of water rotation in the eddy is about 1 m/s. (In some cases, this velocity can reach a value of 3 m/s.) The mean life span of a frontal eddy is a few years, its diameter is reduced in the course of time, and the eddy itself descends with a speed of nearly 0.6 m/day. The structure of the cyclonic eddies of the open ocean coincides qualitatively with that of the frontal eddies. However, the former have a smaller diameter and lower velocity of rotation.

Currents can also be caused by tides and internal gravity waves. The velocity of water motion in tides and internal gravity waves can reach a value of 1 m/s and a few tens of cm/s, respectively. The vertical velocity of water motion caused by an internal gravity wave may not be ignored.

1.3.2 Effects of currents on sound propagation

A typical variation of the sound speed in the ocean is $|c - c_0|/c_0 \sim 3 \times 10^{-2}$, where c_0 is a reference value of the sound speed c. On the other hand, the ratio v/c is of the order of 10^{-3} (i.e., 30 times smaller than the typical value of $|c - c_0|/c_0$), even for strong currents with $v \sim 1.5$ m/s. Nevertheless, currents can affect sound propagation as a result of at least three mechanisms.

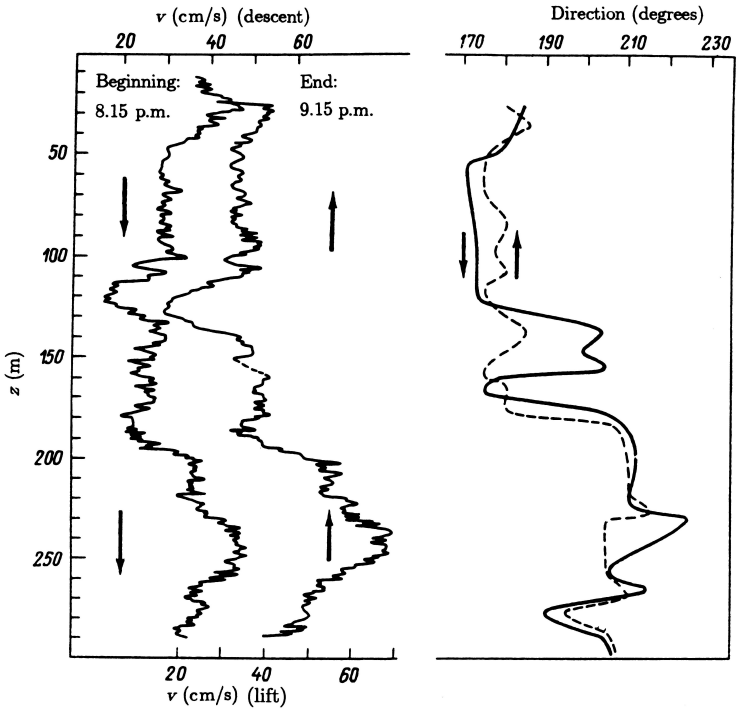

FIGURE 1.6
Magnitude and direction of current velocity measured by descent (↓) and lift (↑) of a quick-response probe [260].

First, currents can change the phase of a sound wave, and hence its travel time, if the propagation range is sufficiently large. It follows from equation (3.97) that the phase change caused by a current is given by $\Delta\Phi \approx -2\pi f R\bar{v}_R/c^2$. Here, R is the distance from the source to the receiver, f is the acoustic frequency, and $\bar{v}_R$ is the mean value (along the sound path) of the current velocity component $v_R(z)$ in the direction from the source to the receiver. This phase change is significant if $|\Delta\Phi| \gtrsim \pi/8$. Substituting the value of $\Delta\Phi$ into this inequality yields

$$R \gtrsim \frac{c^2}{16 f \bar{v}_R}. \tag{1.4}$$

Currents can contribute significantly to the phase change of a sound field if R satisfies the latter inequality. If $\bar{v}_R = 0.3$ m/s and $f = 100$ Hz, it follows from equation (1.4) that $R \gtrsim 4.7$ km.

Second, currents can cause a noticeable change in the amplitude of a sound field. Indeed, if two or more sound rays arrive at the observation point, and

the phase change along at least one of the rays depends on $\bar{v}_R$, the amplitude of the resulting sound field also depends on $\bar{v}_R$. Note that the effect of $\bar{v}_R$ on the sound-pressure amplitude along a sound ray can usually be ignored.

Third, currents can lead to a qualitative change of sound propagation if $|\partial v/\partial z| \gtrsim |\partial c/\partial z|$.

In the remaining part of this section, we shall consider these effects for sound propagation through currents, synoptic eddies, and tides.

1.3.3 Currents

It has been shown that the currents can cause a significant change in the amplitude and phase of a sound field and its travel time [120, 364]. The profiles of $c(z)$ and $v(z)$ have been assumed to be linear or constant, and the sound field has been calculated using geometrical acoustics (see section 3.5).

Sound propagation in the direction of water motion in the Gulf Stream and in the opposite direction has been studied theoretically [149]. In these cases, the ocean can be considered a stratified moving medium. Figure 1.7 shows the vertical profiles of $c(z)$ and $v(z)$ that were adopted for the calculation of the sound field [149]. These profiles are typical of the Gulf Stream, where the ocean depth is large. It was assumed that the source and receiver are located at a depth of 250 m and the acoustic frequency is 50 Hz. Calculations were performed using the wave theory (section 4.1) and the effective sound speed c_{eff}, as defined with equation (1.3). The predicted sound intensity I versus the horizontal range r is shown in figure 1.8 for sound propagation in the direction of the current and in the opposite direction.

In this numerical example, $|\partial v/\partial z| > |\partial c/\partial z|$ for $z \lesssim 0.5$ km. As a result, sound propagation in the direction of the current differs qualitatively from that in the opposite direction. In the direction of the current and for $z \lesssim 0.5$ km, the value of c_{eff} decreases if the depth is increased, so that there is an antiwaveguide sound propagation and a shadow zone exists at a horizontal range 20 km $\lesssim r \lesssim$ 50 km (see figure 1.8). But in the opposite direction, there is a waveguide near the ocean surface because c_{eff} increases with depth for $z \lesssim 0.5$ km. This waveguide contains one acoustic mode. Because of the mode, the sound intensity I is greater than that in the direction of the current by 15 dB. Since the profiles of $c(z)$ and $v(z)$ that have been adopted for calculations [149] are model profiles, it would be of interest to carry out experiments to confirm that the currents can qualitatively change the sound propagation in the ocean. (See also section 3.5.3.)

The effect of a geostrophic flow on sound propagation in the shallow ocean has been studied [119, 121]. To this end, a model of a geostrophic flow has been developed [121]. It is assumed in this model that the current velocity decreases linearly with depth and is directed to the north. Owing to a geostrophic balance, there is a horizontal gradient of the sound speed c in the eastern direction, which depends on the current velocity v_s at the ocean surface. The dependence of c on z is linear. This model of a geostrophic flow describes

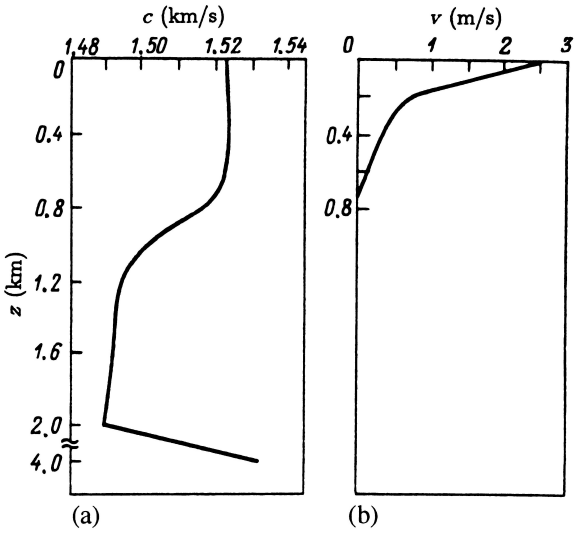

FIGURE 1.7
Vertical profiles of (a) sound speed and (b) current velocity used for calculation of the sound field [149] shown in figure 1.8.

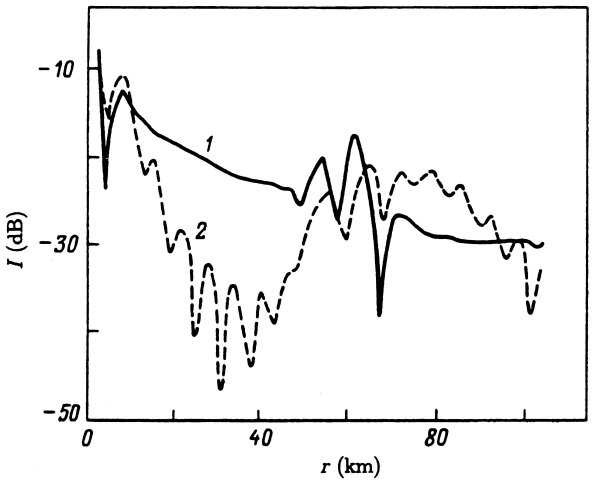

FIGURE 1.8
Sound intensity I versus horizontal range r for the profiles $c(z)$ and $v(z)$ shown in figure 1.7 [149]. Lines 2 and 1 correspond to sound propagation in the direction of the current and in the opposite direction, respectively.

approximately the profiles of c and $\mathbf{v}$ of the Gulf Stream in the Florida Strait. Sound propagation perpendicular to the axis of a geostrophic flow has been considered [119]. It has been shown that, to an accuracy of v/c, the current does not directly affect the sound field in the geometrical acoustics approximation. However, a variation of v_s causes a variation of $c(\mathbf{r}, z)$ (because the horizontal gradient of c depends on v_s) and, hence, a change of the sound field. Calculations [119] have shown that the phase change of a sound field depends linearly on the variation of v_s. This result is in good agreement with the experimental data [119] on sound propagation from Miami, Florida, to Bimini, Bahamas, perpendicular to the Florida Strait.

1.3.4 Synoptic eddies

Let us now consider the effects of water motion in synoptic eddies on sound propagation. Model profiles of the sound speed $c(r, z)$ and current velocity $\mathbf{v}(r, z)$ in the synoptic eddies have been constructed [163]. These profiles have been used for studying sound propagation through the synoptic eddies over horizontal ranges of few tens of kilometers [162, 179] and 1000 km [180]. This work has shown that the amplitude and phase of a sound field are affected mainly by variation of the sound speed in the eddy. Nevertheless, the water motion in the eddy can cause a sound intensity variation greater than 10–12 dB, and a phase change much greater than π. Thus, the effects of water motion on sound propagation should be taken into account if a sound wave passes through a synoptic eddy.

1.3.5 Tides

The effect of tidal currents on sound propagation in the shallow ocean has been considered [363]. It has been assumed that c and v do not depend on the spatial coordinates and that v varies slowly with time. It has been predicted that the sound-pressure amplitude depends on the current velocity significantly and that its phase is proportional to v_R. The linear dependence of the phase on v_R has been confirmed by measuring sound propagation between Block Island, Rhode Island, and Fishers Island, New York.

1.3.6 Reciprocal acoustic transmission

It has been argued above that the motion of oceanic water caused by currents, synoptic eddies, and tides can affect sound propagation significantly. Reciprocal transmission paths (parallel paths that are in close proximity, but in opposite directions) can be used to study this effect experimentally. Indeed, it is difficult to separate the effect of currents on a sound field from the effect of sound speed variations on the same sound field if sound signals propagate only in one direction. According to the reciprocity principle, sound signals propagating in opposite directions totally coincide if $\mathbf{v} = 0$, but they are different

if $\mathbf{v} \neq 0$. Reciprocal acoustic transmission has been studied experimentally [266]. In reference [436], an experiment was described in which two sources were located at a depth of 1 km and the horizontal distance between them was 25 km. This experiment showed that the travel time of the sound impulse, its amplitude, and its shape depend significantly on the direction of sound propagation.

Currents can be reconstructed using reciprocal transmission and measuring the difference in the travel time of impulse propagation in opposite directions. Such a remote sensing technique would enable scientists to investigate the structures of unsteady currents, synoptic eddies, tides, and internal gravity waves. The significance of this application has resulted in several publications [271, 335, 336] where the effects of currents on reciprocal transmission have been studied numerically using the parabolic equation method. The results obtained in these papers show that currents can affect the amplitude, phase, and travel time of sound transmissions.

2

Equations for acoustic and internal gravity waves in an inhomogeneous moving medium

In this chapter, the equations for acoustic and internal gravity waves in inhomogeneous moving media are systematically derived and analyzed. The ranges of applicability of these equations are studied in detail and they are compared with results presented previously in the literature. The equations in this chapter are used in subsequent chapters for studies of sound propagation in moving media.

In section 2.1, a complete set of fluid dynamic equations is presented. These equations are then linearized resulting in a set of linearized equations of fluid dynamics which provides the most general description of both acoustic and internal gravity waves in a moving medium. The set of linearized equations is, however, rather involved for analytical or numerical studies of sound propagation. In a stratified moving medium (sections 2.2 and 2.3), this set reduces exactly to a single equation for the pressure of an acoustic or internal gravity wave, which is more convenient for analysis. In a three-dimensional moving medium (section 2.4), with some approximations, the linearized equations of fluid dynamics reduce to two coupled equations for the sound pressure and acoustic particle velocity. Using additional approximations, these coupled equations reduce to wave-type and Helmholtz-type equations for the sound pressure. In section 2.5, narrow-angle and wide-angle parabolic wave equations are derived, which are convenient for both analytical and numerical studies of sound propagation in a three-dimensional moving medium.

The flowchart of the most important equations considered in this chapter is shown in figure 2.1. It also provides with the ranges of applicability of these equations and indicates where they are used.

In this chapter, we also consider equations for the pressure, density, medium velocity, entropy, and concentrations of the components dissolved in the medium through which acoustic and internal gravity waves propagate. Section 2.1 presents such equations for a three-dimensional moving medium and section 2.2 for a stratified moving medium.

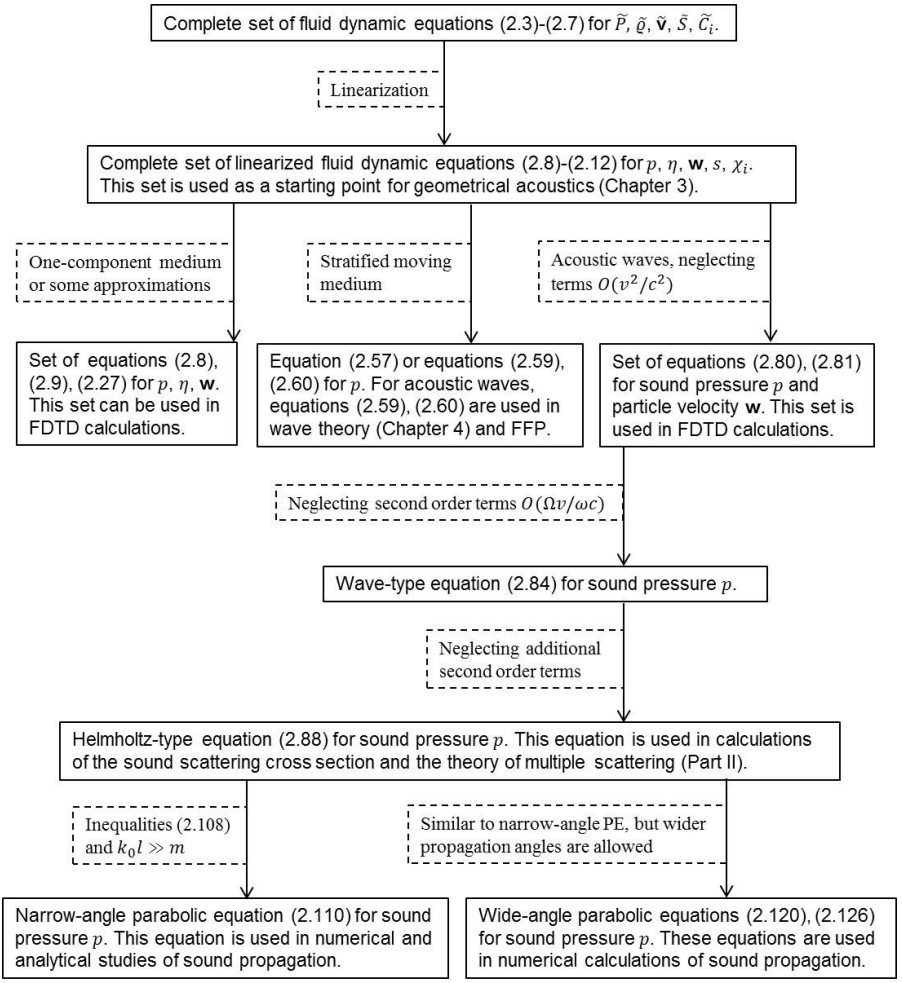

FIGURE 2.1
Flowchart of the most important equations considered in Chapter 2. Dashed boxes adjacent to the arrows indicate approximations/assumptions made in the derivations. $\widetilde{P}$, $\widetilde{\varrho}$, $\widetilde{\mathbf{v}}$, $\widetilde{S}$, and $\widetilde{C}_i$ are the total pressure, density, velocity, entropy, and the concentrations of the components dissolved in the medium; p, η, $\mathbf{w}$, s, and χ_i are their fluctuating components due to a propagating wave. FDTD stands for the finite-difference, time-domain method and FFP for the fast-field program.

2.1 Fluid dynamic equations and their linearization

2.1.1 Fluid dynamic equations

The most general possible approach to wave propagation in an inhomogeneous moving medium is based on the complete set of fluid dynamic equations:

$$\left(\frac{\partial}{\partial t} + \widetilde{\mathbf{v}} \cdot \nabla\right) \widetilde{\varrho}_i + \widetilde{\varrho}_i \nabla \cdot \widetilde{\mathbf{v}} = \widetilde{\varrho}_i Q, \quad i = 0, 1, \ldots, n, \tag{2.1}$$

$$\widetilde{P} = \widetilde{P}(\widetilde{S}, \widetilde{\varrho}_0, \widetilde{\varrho}_1, \ldots, \widetilde{\varrho}_n), \tag{2.2}$$

$$\left(\frac{\partial}{\partial t} + \widetilde{\mathbf{v}} \cdot \nabla\right) \widetilde{\mathbf{v}} + \frac{1}{\widetilde{\varrho}} \nabla \widetilde{P} - \mathbf{g} = \mathbf{F}, \tag{2.3}$$

$$\left(\frac{\partial}{\partial t} + \widetilde{\mathbf{v}} \cdot \nabla\right) \widetilde{S} = 0. \tag{2.4}$$

Here, $\widetilde{P}(\mathbf{R}, t)$ is the pressure in the medium, $\widetilde{\varrho}_i(\mathbf{R}, t)$ are the densities of the components of the medium, $\widetilde{\mathbf{v}}(\mathbf{R}, t)$ is the velocity vector, and $\widetilde{S}(\mathbf{R}, t)$ is the entropy, where $\mathbf{R} = (x, y, z)$ are the Cartesian coordinates and t is time. In equations (2.1)–(2.4), $\widetilde{\varrho} = \sum_{i=0}^{n} \widetilde{\varrho}_i$ is the total density of the medium, $\nabla = (\partial/\partial x, \partial/\partial y, \partial/\partial z)$, $\mathbf{g} = (0, 0, -g)$ the vector of the acceleration due to gravity (the direction of this vector is opposite to the direction of the vertical z-axis), and $\mathbf{F}(\mathbf{R}, t)$ and $Q(\mathbf{R}, t)$ characterize a force acting on the medium and a mass source, respectively. The tilde above the quantities $\widetilde{P}$, $\widetilde{\varrho}_i$, $\widetilde{\mathbf{v}}$, and $\widetilde{S}$ indicates that the medium is perturbed by a wave propagating through it. Equations (2.1)–(2.4) express, respectively, the law of mass conservation of the ith component of the medium, the equation of state, the law of momentum conservation, and the assumption of adiabatic motion of the medium. We consider that a medium consists of $n + 1$ components with densities $\widetilde{\varrho}_i$ since these components can affect sound propagation. For example, in the ocean, the sound speed depends on the concentration of salt dissolved in the water; in the atmosphere, fluctuations of water vapor cause fluctuations of the sound field.

Instead of the densities $\widetilde{\varrho}_0, \widetilde{\varrho}_1, \ldots, \widetilde{\varrho}_n$, it is convenient to deal with the total density $\widetilde{\varrho}$ of the medium and the concentrations $\widetilde{C}_i = \widetilde{\varrho}_i / \widetilde{\varrho}_0$ of the components dissolved in the medium. Here, $\widetilde{\varrho}_0$ is the density of the basic component of the medium (the basic solvent) and the index i is redefined as $i = 1, 2, \ldots, n$. In this case, equations (2.1) and (2.2) take the form

$$\left(\frac{\partial}{\partial t} + \widetilde{\mathbf{v}} \cdot \nabla\right) \widetilde{\varrho} + \widetilde{\varrho} \nabla \cdot \widetilde{\mathbf{v}} = \widetilde{\varrho} Q, \tag{2.5}$$

$$\left(\frac{\partial}{\partial t} + \widetilde{\mathbf{v}} \cdot \nabla\right) \widetilde{C}_i = 0, \quad i = 1, 2, \ldots, n, \tag{2.6}$$

$$\widetilde{P} = \widetilde{P}(\widetilde{\varrho}, \widetilde{S}, \widetilde{C}_1, \widetilde{C}_2, \ldots, \widetilde{C}_n). \tag{2.7}$$

Equations (2.3)–(2.7) represent a complete set of equations for $\widetilde{P}$, $\widetilde{\varrho}$, $\widetilde{\mathbf{v}}$, $\widetilde{S}$, and $\widetilde{C}_i$. This set is referenced at the top of the flowchart of equations depicted in figure 2.1.

2.1.2 Linearized equations of fluid dynamics

For describing a wave propagating in the medium, in equations (2.3)–(2.7) we set $\widetilde{P} = P + p$, $\widetilde{\varrho} = \varrho + \eta$, $\widetilde{\mathbf{v}} = \mathbf{v} + \mathbf{w}$, $\widetilde{S} = S + s$, and $\widetilde{C}_i = C_i + \chi_i$. Here, P, ϱ, $\mathbf{v}$, S, and C_i are the ambient values (i.e., the values in the absence of a propagating wave) of the pressure, density, medium velocity, entropy, and the concentrations of the components dissolved in the medium, and p, η, $\mathbf{w}$, s, and χ_i are their fluctuations due to a propagating wave. All these quantities are functions of both $\mathbf{R}$ and t. In many cases, the wave propagating in the medium disturbs this medium only slightly. In such cases, equations (2.3)–(2.7) can be linearized with respect to p, η, $\mathbf{w}$, s, and χ_i. Rearranging the resulting linearized equations, we obtain

$$\frac{d\mathbf{w}}{dt} + (\mathbf{w}\cdot\nabla)\mathbf{v} + \frac{1}{\varrho}\nabla p - \frac{\eta\nabla P}{\varrho} = \mathbf{F}, \tag{2.8}$$

$$\frac{d\eta}{dt} + (\mathbf{w}\cdot\nabla)\varrho + \varrho\nabla\cdot\mathbf{w} + \eta\nabla\cdot\mathbf{v} = \varrho Q, \tag{2.9}$$

$$\frac{d\chi_i}{dt} + (\mathbf{w}\cdot\nabla)C_i = 0, \quad i = 1, 2, \ldots, n, \tag{2.10}$$

$$\frac{ds}{dt} + (\mathbf{w}\cdot\nabla)S = 0, \tag{2.11}$$

$$p = c^2\eta + hs + b_i\chi_i. \tag{2.12}$$

Here, the operator $d/dt = \partial/\partial t + \mathbf{v}\cdot\nabla$ is the full (material) derivative, repeated subscripts are summed from 1 to 3, $c^2 = \partial P/\partial\varrho$ is the square of the sound speed, $h = \partial P/\partial S$, and $b_i = \partial P/\partial C_i$. Hereafter, when calculating the partial derivatives of the ambient pressure P, we assume that P is a function of the thermodynamic variables ϱ, S, C_1, C_2,..., C_n (see equation (2.17) below). These thermodynamic variables are convenient for derivations of equations for acoustic and internal gravity waves. When deriving equations (2.8) and (2.9), we assumed that $\mathbf{F}$ and Q are of the same order of magnitude as p, η, $\mathbf{w}$, s, and χ_i. In other words, $\mathbf{F}$ and Q are the sources of waves propagating in the medium. The ambient quantities P, ϱ, $\mathbf{v}$, S, and C_i satisfy the set of equations (2.3)–(2.7) with $\mathbf{F} = Q = 0$. Rearranging these equations, we have

$$\frac{d\mathbf{v}}{dt} + \frac{1}{\varrho}\nabla P - \mathbf{g} = 0, \tag{2.13}$$

$$\frac{d\varrho}{dt} + \varrho\nabla\cdot\mathbf{v} = 0, \tag{2.14}$$

$$\frac{dC_i}{dt} = 0, \quad i = 1, 2, \ldots, n, \tag{2.15}$$

$$\frac{dS}{dt} = 0, \tag{2.16}$$

$$P = P(\varrho, S, C_1, C_2, \ldots, C_n). \tag{2.17}$$

The complete set of the linearized equations of fluid dynamics, equations (2.8)–(2.12), provides the most general description of wave propagation in an inhomogeneous moving medium. In order to calculate p, η, $\mathbf{w}$, s, and χ_i, one needs to know the ambient quantities P, ϱ, $\mathbf{v}$, S, and C_i. This set describes the propagation of both acoustic and internal gravity waves. We shall study these waves simultaneously where it is possible (in this and following sections). All equations for wave propagation in a moving medium are derived in this chapter from the set of equations (2.8)–(2.12). This set is also used in Chapter 3 as a starting point in the formulations of the geometrical acoustics. It is referenced close to the top in the flowchart of equations in figure 2.1. Equations (2.8)–(2.12) were first derived by Blokhintzev (sections 4 and 13 in reference [37]).

2.1.3 Set of three coupled equations

With some assumptions or approximations, equations (2.8)–(2.12) can be reduced to a set of three coupled equations for p, η, and $\mathbf{w}$. To this end, we apply the operator d/dt to both sides of equation (2.12). In the resulting equation, $d\chi_i/dt$ and ds/dt are expressed in terms of $\mathbf{w}$ using equations (2.10) and (2.11), respectively. As a result, we have

$$\frac{dp}{dt} = c^2\frac{d\eta}{dt} + \eta\frac{dc^2}{dt} + s\frac{dh}{dt} + \chi_i\frac{db_i}{dt} - h\mathbf{w}\cdot\nabla S - b_i\mathbf{w}\cdot\nabla C_i. \tag{2.18}$$

The full derivative dc^2/dt appearing in this equation is recast in the form:

$$\frac{dc^2}{dt} = \frac{d}{dt}\frac{\partial P}{\partial \varrho} = \frac{\partial^2 P}{\partial \varrho^2}\frac{d\varrho}{dt} + \frac{\partial^2 P}{\partial S \partial \varrho}\frac{dS}{dt} + \frac{\partial^2 P}{\partial C_i \partial \varrho}\frac{dC_i}{dt} = \beta\frac{d\varrho}{dt}, \tag{2.19}$$

where $\beta = \partial^2 P/\partial \varrho^2$. In equation (2.19), we took into account that $dS/dt = dC_i/dt = 0$ (see equations (2.15) and (2.16)). Analogously, we can derive equations for dh/dt and db_i/dt:

$$\frac{dh}{dt} = \alpha\frac{d\varrho}{dt}, \quad \frac{db_i}{dt} = \tau_i\frac{d\varrho}{dt}, \tag{2.20}$$

where $\alpha = \partial^2 P/\partial \varrho \partial S$ and $\tau_i = \partial^2 P/\partial \varrho \partial C_i$.

We apply the operator $\mathbf{w}\cdot\nabla$ to both sides of the equation of state (2.17). Taking into account the definitions of c^2, h, and b_i, we obtain

$$\mathbf{w}\cdot\nabla P = c^2\mathbf{w}\cdot\nabla\varrho + h\mathbf{w}\cdot\nabla S + b_i\mathbf{w}\cdot\nabla C_i. \tag{2.21}$$

Substituting the values of dc^2/dt, dh/dt, and db_i/dt into this equation and, then, adding equations (2.18) and (2.21), we have

$$\frac{dp}{dt} + \mathbf{w} \cdot \nabla P = c^2 \frac{d\eta}{dt} + c^2 \mathbf{w} \cdot \nabla \varrho + \tilde{c}^2 \frac{d\varrho}{dt}, \tag{2.22}$$

where $\tilde{c}^2 = \beta\eta + \alpha s + \tau_i \chi_i$. It can be shown that $\tilde{c}^2$ represents fluctuations in the sound speed squared, caused by a wave propagating in the medium. In the equation for $\tilde{c}^2$, we replace s with its value obtained from equation (2.12): $s = (p - c^2\eta - b_i\chi_i)/h$. As a result, we obtain the expression for $\tilde{c}^2$:

$$\tilde{c}^2 = \frac{1}{h}\left[\left(h\beta - \alpha c^2\right)\eta + \alpha p + \Omega\chi_i\right], \tag{2.23}$$

where Ω is given by:

$$\Omega = h\tau_i - \alpha b_i = \frac{\partial P}{\partial S}\frac{\partial^2 P}{\partial \varrho \partial C_i} - \frac{\partial P}{\partial C_i}\frac{\partial^2 P}{\partial \varrho \partial S}. \tag{2.24}$$

We multiply equation (2.9) by c^2, add the resulting equation and equation (2.22), and replace $d\varrho/dt$ with $-\varrho\nabla \cdot \mathbf{v}$ using equation (2.14). As a result, we have

$$\frac{dp}{dt} + \varrho c^2 \nabla \cdot \mathbf{w} + \mathbf{w} \cdot \nabla P + \left(c^2\eta + \varrho\tilde{c}^2\right)\nabla \cdot \mathbf{v} = 0. \tag{2.25}$$

Substituting for $\tilde{c}^2$ using equation (2.23), we arrive at the following equation for dp/dt:

$$\frac{dp}{dt} + \varrho c^2 \nabla \cdot \mathbf{w} + \mathbf{w} \cdot \nabla P + \left\{\left[\varrho\beta + c^2(1 - \alpha\varrho/h)\right]\eta + (\alpha\varrho/h)\,p + (\varrho\Omega/h)\chi_i\right\}\nabla \cdot \mathbf{v} = \varrho c^2 Q. \tag{2.26}$$

This equation is an exact consequence of the linearized equations of fluid dynamics (2.8)–(2.12). It contains the following unknown functions: p, η, $\mathbf{w}$, and χ_i.

Now let us omit the term $(\varrho\Omega/h)\chi_i$ appearing on the left-hand side of equation (2.26), the justification for which is discussed later. Then, this equation simplifies to [303]:

$$\frac{dp}{dt} + \varrho c^2 \nabla \cdot \mathbf{w} + \mathbf{w} \cdot \nabla P + \left\{\left[\varrho\beta + c^2(1 - \alpha\varrho/h)\right]\eta + (\alpha\varrho/h)\,p\right\}\nabla \cdot \mathbf{v} = \varrho c^2 Q. \tag{2.27}$$

Equations (2.8), (2.9), and (2.27) comprise a desired set of three coupled equations for p, η, and $\mathbf{w}$. This set describes propagation of both acoustic and internal gravity waves. In the set, one needs to know the following ambient quantities: c, ϱ, $\mathbf{v}$, and P; the coefficients α, β, and h can be calculated

with the equation of state (2.17). Equation (2.27) has been derived from the linearized equations of fluid dynamics assuming that $(\varrho\Omega/h)\chi_i = 0$. This assumption is valid if the medium consists of only one component ($C_i = \chi_i = 0$) or if $\Omega = 0$. The latter equality might hold for a particular medium; for example, it is valid for the medium consisting of two components with the equation of state $P(\varrho, S, C) = f_1(\varrho)f_2(S)f_3(C)$. Note that, generally, $\Omega \neq 0$. If neither of the equalities $C_i = 0$ and $\Omega = 0$ are valid, the set of equations (2.8), (2.9), and (2.27) describes approximately propagation of acoustic and internal gravity waves. This set can potentially be used for finite-difference, time-domain (FDTD) calculations of wave propagation in a moving medium, which are performed typically with partial differential equations that are first order in time. Figure 2.1 shows this set in the flowchart of equations.

Equation (2.27) can be simplified for an ideal gas. In this case, the equation of state is given by:

$$P = P_0(\varrho/\varrho_0)^\gamma \exp[(\gamma - 1)\mu(S - S_0)/R], \tag{2.28}$$

where R is the universal gas constant, μ is the molecular weight of the gas, $\gamma = c_P/c_V$ is the ratio of the specific heat at constant pressure c_P to the specific heat at constant volume c_V, and P_0, ϱ_0, and S_0 are the reference values of the corresponding ambient quantities. Using equation (2.28), the sound speed c and the coefficients α, β, and h appearing in equation (2.27) can be calculated: $c^2 = \gamma P/\varrho$, $\alpha = \gamma(\gamma - 1)\mu P/(\varrho R)$, $\beta = \gamma(\gamma - 1)P/\varrho^2$, and $h = (\gamma - 1)\mu P/R$. Substituting these values into equation (2.27), we have

$$\frac{dp}{dt} + \varrho c^2 \nabla \cdot \mathbf{w} + \mathbf{w} \cdot \nabla P + \gamma p \nabla \cdot \mathbf{v} = \varrho c^2 Q. \tag{2.29}$$

Equations (2.8), (2.9), and (2.29) together provide a complete set of three coupled equations for p, η, and $\mathbf{w}$ for the case of an ideal gas. To solve these equations, one needs to know the following ambient quantities: c, ϱ, $\mathbf{v}$, and P. With some approximations [303], this set can be reduced to the set of two coupled equations for p and $\mathbf{w}$ which was used in reference [346] for FDTD calculations of sound propagation in the atmosphere.

2.1.4 Energy considerations

Generally, a linear wave propagating in an inhomogeneous moving medium can exchange energy with the ambient medium so that the wave energy is not conserved. Indeed, in fluid dynamics, the law of energy conservation has the form

$$\frac{\partial}{\partial t}(\widetilde{\varrho}\,\widetilde{v}^2/2 + \widetilde{\Xi}) + \nabla \cdot \left[\widetilde{\varrho}\,\widetilde{\mathbf{v}}(\widetilde{v}^2/2 + \widetilde{P}/\widetilde{\varrho} + \widetilde{\Xi})\right] = 0, \tag{2.30}$$

where $\widetilde{\Xi}$ is the internal energy. Let $\widetilde{P} = P + p + p_2 + \ldots$, $\widetilde{\varrho} = \varrho + \eta + \eta_2 + \ldots$, $\widetilde{\mathbf{v}} = \mathbf{v} + \mathbf{w} + \mathbf{w}_2 + \ldots$, and $\widetilde{\Xi} = \Xi + \varepsilon + \varepsilon_2 + \ldots$. The first two terms in

these series have been introduced above (except for Ξ and ε) and describe the ambient medium and a linear wave propagating through the medium. The third terms p_2, η_2, w_2, and ε_2 describe a weakly nonlinear wave; note that $p_2 \sim p^2$, $\eta_2 \sim \eta^2$, $w_2 \sim w^2$, and $\varepsilon_2 \sim \varepsilon^2$. In the absence of a wave propagating in the medium, equation (2.30) takes the form

$$\frac{\partial}{\partial t}(\varrho v^2/2 + \Xi) + \nabla \cdot \left[\varrho \mathbf{v}(v^2/2 + \Xi + P/\varrho)\right] = 0. \tag{2.31}$$

The most consistent approach for deriving the law of energy conservation would be to subtract this equality from equation (2.30) and then to neglect terms of the order of p^3, η^3, w^3, and ε^3. The resulting equation would, however, contain not only the quantities p, η, and $\mathbf{w}$ characterizing a linear wave, but also the quantities p_2, η_2, $\mathbf{w}_2$, and ε_2, which are not considered in the linear theory.

Thus, generally, it is not possible to formulate a law of energy conservation and, hence, to define the energy density and its flux in a wave propagating in an inhomogeneous moving medium. Such a law can be derived only with certain assumptions about a moving medium or a propagating wave. In section 3.1, the law of acoustic energy conservation is formulated in the approximation of geometrical acoustics.

2.1.5 Reduction of the linearized equations of fluid dynamics to a single equation

The complete set of linearized equations of fluid dynamics, equations (2.8)–(2.12), describes, in principle, the propagation of acoustic and internal gravity waves in moving media. However, this set is rather involved and inconvenient for solving particular problems. In the general case of an inhomogeneous moving medium, equations (2.8)–(2.12) cannot be exactly reduced to a single equation, which would be more convenient for analysis.

Equations (2.8)–(2.12) can be reduced exactly to a single equation if we make certain assumptions about the ambient quantities P, ϱ, $\mathbf{v}$, S, and C_i. Such exact equations are the Andreev–Rusakov–Blokhintzev equation (section 2.4), derived assuming that $g = 0$, $S =$ constant, and $\operatorname{rot} \mathbf{v} = 0$; the Goldstein equation for sound waves in a parallel shear flow (section 2.3); and the equation for acoustic and internal gravity waves in a stratified moving medium, derived by Ostashev [281, 283] and considered in detail in section 2.3. Moreover, the set of equations (2.8)–(2.12) can be simplified or reduced to a single equation using various approximations. The approximate equations for sound waves in a three-dimensional moving medium are considered in sections 2.4 and 2.5.